ELSEVIER

Solar Energy Materials & Solar Cells 62 (2000) 97–108

Solar Energy Materials & Solar Cells

www.elsevier.com/locate/solmat

Intrinsic microcrystalline silicon: A new material for photovoltaics

O. Vetterl, F. Finger*, R. Carius, P. Hapke, L. Houben, O. Kluth, A. Lambertz, A. Mück, B. Rech, H. Wagner

Institut für Schicht- und Ionentechnik, ISI-PV, Forschungszentrum Jülich, D-52425 Jülich, Germany

Abstract

Microcrystalline silicon (μc-Si:H) prepared by plasma-enhanced chemical vapor deposition (PECVD) has been investigated as material for absorber layers in solar cells. The deposition process has been adjusted to achieve high deposition rates and optimized solar cell performance. In particular, already moderate variations of the crystalline vs. amorphous volume fractions were found to effect the electronic material – and solar cell properties. Such variation is readily achieved by changing the process gas mixture of silane to hydrogen. Best cell performance was found for material near the transition to the amorphous growth regime. With this optimized material efficiencies of 7.5% for a 2 μm thick μc-Si:H single solar cell and 12% for an a-Si:H/μc-Si:H stacked solar cell have been achieved.

Keywords: Microcrystalline silicon; Solar cells; Deposition rate

1. Introduction

For the choice of photovoltaic materials is valid what can be considered a sentence of believe of the semiconductor industry: if it can be done in silicon, it will be done in silicon. Silicon is abundant, environmentally inert and is one of the technically and scientifically most advanced materials. However, standard silicon photovoltaic technology suffers from several drawbacks: the processes are energy consumptive, too much material is wasted during processing, the cells are – for technical limitations – much thicker than what would be needed, and large area and module fabrication is

* Corresponding author. Tel.: +49-2461-612614; fax: +49-2461-613735.
E-mail address: f.finger@fz-juelich.de (F. Finger)

0927-0248/00/$ - see front matter
PII: S0927-0248(99)00140-3

awkward. On the other hand, conversion efficiencies are high and as mentioned above, the technology is well advanced. Therefore, it has ever been the challenge to improve on those drawbacks while keeping the silicon advantages. One way is the so-called thin film silicon solar cell on glass. With this device one wants to reduce film thickness to what is a minimum needed for complete solar light absorption, reduce process temperatures in order to use low-cost substrate materials and use processes which allow large area fabrication and integration into modules. This is where microcrystalline silicon (μc-Si:H) prepared by plasma-enhanced chemical vapour deposition (PECVD) enters. Being in the field for long in amorphous silicon-based devices as highly conductive contact layer, recently much progress has been made to control the process of fabrication in order to achieve improved deposition rates and high electronic quality such that now μc-Si:H can be used as active layer in solar cells [1–4]. The present approach is to use μc-Si:H as a low band gap red absorber together with an amorphous silicon to cell in a tandem (or tripel) cell design. To be able to further reduce the layer thickness, light scattering becomes important, which is also subject of ongoing research [5,6].

The present paper addresses aspects of the physics and technology of intrinsic PECVD microcrystalline silicon. Material properties as well as the performance of solar cells based on μc-Si:H are discussed.

2. Experimental details

μc-Si:H films and solar cells were prepared in a multichamber PECVD deposition system with separate diode-type parallel plate reactors for doped and undoped layers at a plasma excitation frequency of 95 MHz. The substrate temperature was 200°C, the deposition pressure 300 mTorr. Plasma powers between 5 and 50 W have been employed. The deposition feed gas for the undoped absorber layers was 2–8% silane (SiH_4) in hydrogen (H_2). Doping was achieved by gas admixture of phosphine (PH_3) for the deposition of n-type layers and trimethylboron ($B(CH_3)_3$) for p-type layers. To examine possible effects of oxygen contamination i-layers were prepared with and without use of a gas purifier.

ZnO covered glass serves as substrate for the μc-Si:H *pin* solar cells. The ZnO films were prepared by magnetron sputtering. Distinct light scattering properties were obtained by texture-etching the ZnO surface in diluted HCl [5,6]. As back reflector and contact a ZnO/Ag film system was used, also defining the solar cell area of 1 cm^2. The pin structure consists of an approximately 20 nm thick microcrystalline p-layer, the microcrystalline i-layer and a 30 nm thick amorphous n-layer. For the μc-Si:H *nip* solar cells a texture etched ZnO/Ag double layer sputtered on glass serves as diffuse backreflector [5,6]. Here, the solar cell itself is fully microcrystalline with a 50 nm thick n- and a p-layer with a thickness of approximately 20 nm. As top contact a 80 nm thick ZnO film is used, causing a reflection minimum at $\lambda = 500$ nm. An additional silver grid was applied to the front contact to avoid ohmic losses caused by the high sheet resistance of the thin ZnO top contact. Thus, the active area of the nip solar cells is reduced to 0.7 cm^2.

As substrate for the material studies we used glass (Corning 7059) and glass covered with chromium. Crystalline silicon covered with native oxide was used for the ease of investigation by TEM (transmission electron microscopy). The phase composition of the μc-Si:H films was investigated by Raman spectroscopy. To estimate the degree of crystallinity, the intensity ratio $I_{520\ \mathrm{cm}^{-1}}/(I_{480\ \mathrm{cm}^{-1}} + I_{520\ \mathrm{cm}^{-1}})$ was used as a measure of the crystalline volume content. Doping levels and impurity concentrations were monitored by SIMS measurements. The conductivity was measured with a coplanar contact setup under dark (σ_{dark}) and illuminated (σ_{photo}) conditions.

The thickness of films and solar cells was measured with a step profiler. Solar cells were characterized by measuring the I–V characteristics under AM 1.5 illumination and the spectral response.

3. Material properties

One of the most important features of μc-Si:H is its microstructure, e.g. the volume fraction and spatial distribution of amorphous and crystalline phase within the film. Under deposition conditions that favor the formation of a high crystalline volume fraction, films with columnar grains are found (Fig. 1). The crystalline growth starts at nucleation centers near the interface between film and substrate. During the competitive growth between the nucleation centers the diameter of the remaining crystallites increases resulting in a conical shape of the crystallites near the substrate surface. The space between these crystalline grains can be filled with amorphous silicon and/or voids, strongly dependant on the deposition conditions and the substrate [7]. Since there is no grain coalescence at 200°C, from a certain stage on equally fast growing grains form stable grain boundaries and a columnar structure evolves. Characteristics like grain sizes and phase composition are then independent of the film thickness. Disordered network can only be found in the form of grain boundaries between the crystalline columns. Thus the amorphous volume fraction is low. The diameter of the crystalline columns depends on the deposition conditions and increases with increasing plasma excitation frequency [8,9]. The sample displayed in Fig. 1 was prepared at 95 MHz yielding a grain size of approximately 50 nm. However, the material within the columns is not perfectly single crystalline but exhibits a large amount of twin defects [10], thus the size of perfect single-crystalline domains is smaller.

The crystalline volume content of the films can be varied depending on the deposition conditions. An easy way to achieve this is the variation of the silane concentration SC in the source gas mixture [10,11]. Upon increase of the silane concentration from $\sim 2\%$ to 10% the high crystalline volume fraction is maintained initially but drops sharply in a transition region typically around 6–10%. The width and position of this transition is sensitive to the remaining deposition parameters, e.g. the applied plasma power or the plasma excitation frequency. Fig. 2 displays the change in the microstructure of μc-Si:H upon decrease of the crystalline volume fraction. On the left-hand side the highly crystalline structure as discussed before is shown. In the transition from highly crystalline to predominantly amorphous growth the column size decreases while more amorphous phase is

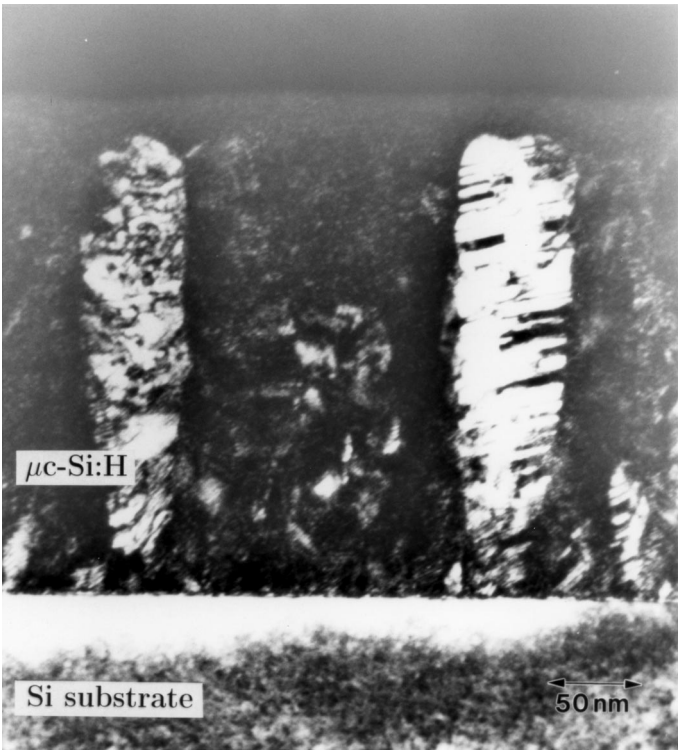

Fig. 1. Dark field transmission electron microscopy micrograph of a μc-Si:H film grown at SC = 2% and a plasma excitation frequency of 95 MHz.

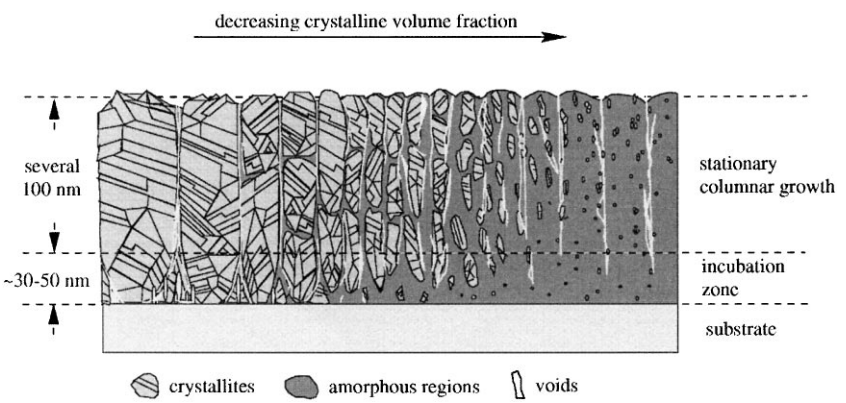

Fig. 2. Schematic diagram showing the prominent microstructural characteristics of μc-Si:H. From the left to the right, the film composition changes from highly crystalline to predominantly amorphous.

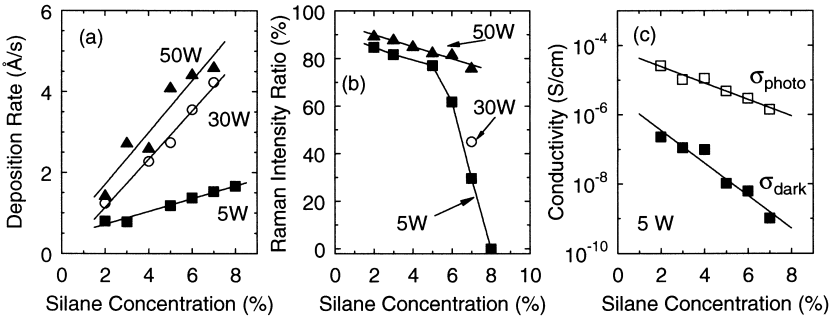

Fig. 3. Properties of μc-Si:H films prepared a various plasma powers and silane concentrations. (a) Deposition rate. (b) Raman intensity ratio $I_c/(I_c + I_a)$. (c) Dark and photo conductivity. Discharge powers of 5 W (■,□), 30 W (○) and 50 W (▲) were used. (after Refs. [4,12]).

incorporated between the crystalline grains, which interrupts the columnar crystalline structure in the lateral direction. Note that the material on the right-hand side of the figure is *not* typical for amorphous silicon used in a-Si:H solar cells, but shows the transition region between μc-Si:H and a-Si:H. This material is characterized by columnar growth of amorphous silicon with very small crystalline domains embedded in the amorphous matrix. It is obvious that the electrical and optical properties of the material will be affected by such structural changes. This is examined in the following for microcrystalline i-layers prepared with different silane concentrations SC in the source gas at different plasma powers.

Changing SC also influences the growth rate of the microcrystalline silicon films. The deposition rate increases with SC especially at high plasma powers of 30 and 50 W (Fig. 3(a)). In Fig. 3(b) the structural composition of the material is described in terms of the intensity ratio $I_{520\ \mathrm{cm}^{-1}}/(I_{480\ \mathrm{cm}^{-1}} + I_{520\ \mathrm{cm}^{-1}})$ in the Raman spectra. This value can be used as a measure for the crystallinity of the films. At a discharge power of 5 W we find the transition to amorphous growth regime at SC of ~5–7%. At 30 and 50 W the transition is at higher SCs, e.g. the sample prepared at 50 W and 7% silane is still highly crystalline. To examine the electrical transport properties the dark conductivity σ_{dark} and photo conductivity σ_{photo} of the 5 W series were measured at room temperature. The results are shown in Fig. 3(c). Both σ_{dark} and σ_{photo} decrease gradually with increasing SC. This applies to the low SC region, where the structural composition of the material changes only little and surprisingly also to the transition region to amorphous growth (see Fig. 2). Since σ_{dark} decreases more than σ_{photo} the photosensitivity $\sigma_{\mathrm{dark}}/\sigma_{\mathrm{photo}}$ increases with SC from 10^2 to 10^3. To investigate whether any residual gas or impurity doping effects are present in our material, as has been suggested by Meier et al. [13], the influence of microdoping and gas purifiers were studied. Neither by boron doping (10^{18}–10^{20} cm^{-3}) nor by reduction of the oxygen content of the film from 10^{19} cm^{-3} to below 10^{18} cm^{-3} the dark conductivity could be further reduced. Therefore the material can be considered as truly intrinsic. Some of the films were characterized by ESR exhibiting a spin density of several 10^{16} cm^{-3} [14]. This is an indication for the good hydrogen passivation of the grain boundary

defects. Interestingly the optical absorption above the gap of the intrinsic μc-Si:H remains largely unchanged upon changes in SC. Only beyond the transition to amorphous growth noticeable changes of the optical absorption are observed.

It is now a question of major importance, in which way differences in the structural composition and the related changes in the electrical and optical properties affect the performance of solar cells with μc-Si:H absorber layers. So far, the connection between these material properties and the solar cell parameters (V_{OC}, FF and j_{SC}) are not understood.

As an example the influence of changes in SC and the discharge power during preparation of the intrinsic μc-Si:H layers on the solar cell performance will be demonstrated in the following. In addition the important aspect of light scattering substrates shall be addressed.

4. Solar cells

For the design of a thin film solar cell using a μc-Si:H the absorber layer thickness is a crucial point. A minimization of the active layer thickness is desirable, because the deposition rates in the PECVD process are a few Å/s (see Fig. 3a). On the other hand, a minimum thickness is required for sufficient absorption of light. Fig. 4 shows the absorption coefficient of intrinsic μc-Si:H as measured by photothermal deflection spectroscopy (PDS). For comparison data of a-Si:H and c-Si are plotted. For energies above 1.7 eV the absorption of μc-Si:H is higher than for c-Si. Possible reasons for this effect include absorption in disordered phase and internal light scattering. For energies below 1.7 eV μc-Si:H and c-Si show similar values for the absorption coefficient α, which means the absorption of μc-Si:H is significantly higher in this region compared to a-Si:H. Thus light with $\lambda > 700$ nm can be absorbed. However,

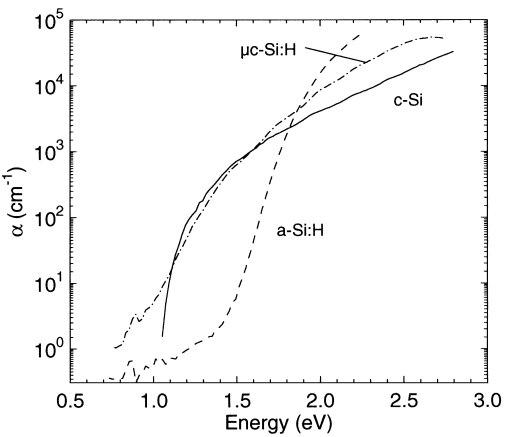

Fig. 4. Absorption coefficient α of single crystalline silicon (c-Si), amorphous silicon (a-Si:H) and microcrystalline silicon (μc-Si:H), as measured by PDS.

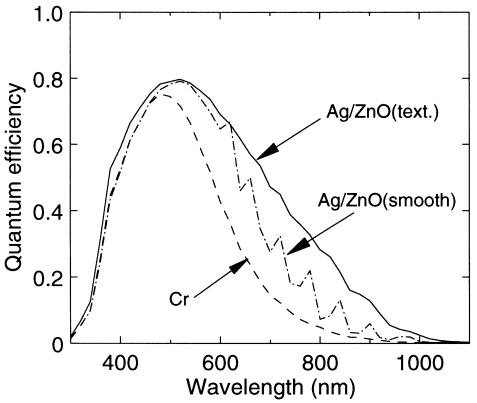

Fig. 5. Quantum efficiency of a *nip* solar cell with 1 μm μc-Si:H absorber layer on different back reflectors as indicated.

α is only 10^2–10^3 cm^{-1}, so that a thickness of several 10 μm is needed for a sufficient absorption. The concept of light trapping solves this problem by lengthening the way of the light through the absorber layer. In the ideal case the light is repeatedly reflected within the multilayered device and is completely absorbed in the μc-Si:H i-layer. An efficient light trapping can be achieved by introducing diffuse scattering by textured front and/or back surfaces. Fig. 5 shows the quantum efficiency of a 1 μm thick μc-Si:H *nip* solar cell with different back reflectors. The chromium back contact gives an estimation of the single pass behavior due to its low reflectivity. A silver back reflector covered with smooth ZnO (note the interference patterns) can enhance the efficiency significantly compared with the chromium back contact. A further increase of performance is achieved by texturing the ZnO. The diffuse scattering lengthens the optical distance traveled by the light within the intrinsic layer by causing multiple reflections and improves the quantum efficiency for $\lambda > 650$ nm further. Comparing the resulting quantum efficiency to the values on the chromium back reflector one can estimate a light trapping factor up to 10 in the long wavelength range ($\lambda > 800$ nm). This means adapted light trapping schemes reduce the required μc-Si:H i-layer thickness from several 10 μm to only several μm.

To examine the effect of intrinsic μc-Si:H absorber layers prepared with different silane concentrations on the solar cells performance a series of 1 μm thick nip devices has been prepared. Fig. 6 shows the solar cell properties (a) efficiency η (b) open-circuit voltage V_{OC} (c) fill factor FF and (d) short-circuit current density j_{SC} as measured under AM 1.5 illumination. As a striking result V_{OC} increases continuously with the silane concentration from 400 mV up to more than 520 mV. This increase in V_{OC} is reflected in the dark I–V characteristics of the solar cells. The diode quality factor stays almost constant, while the saturation current j_0 decreases with increasing SC. This could be related to the observed decrease of the dark conductivity with increasing SC. However, a physical model describing this correlation does not exist up to now.

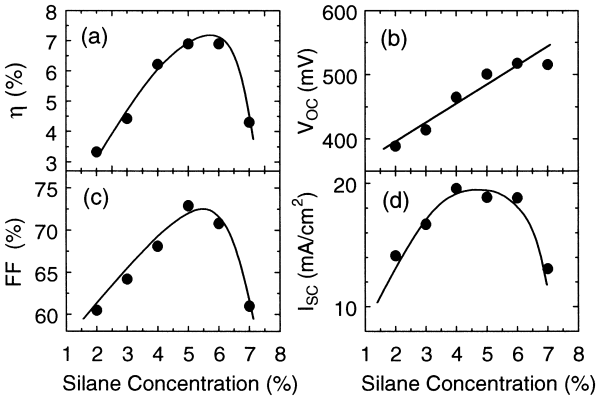

Fig. 6. Results of the I–V measurements of 1 μm thick *nip* solar cells prepared at a plasma power of 5 W (a) efficiency η (b) open-circuit voltage V_{OC} (c) fill factor FF (d) short-circuit current I_{SC}. Lines are guide to the eyes.

Though a higher silane concentration causes the beneficial effect of a higher V_{OC} there is a sudden decrease of FF and j_{SC} when a certain silane concentration is exceeded. At this point the columnar crystalline growth collapses and a noticeable amorphous volume fraction is produced. Deposition conditions with a low silane concentration also lead to a decrease of FF and j_{SC}. The reason for the limitation of carrier extraction in the highly crystalline material is not yet understood. Possible reasons are breakdown of the electrical field, recombination losses (e.g. at poorly passivated grain boundaries) or interface effects between doped and intrinsic layers. As a result of the described trends the combination of highest FF, highest j_{SC} and highest V_{OC} is obtained *near the transition to the amorphous growth regime* yielding an efficiency of 7%. The high current density of nearly 20 mA/cm^2 for a 1 μm absorber thickness is only possible by the use of the highly efficient diffuse scattering backreflector.

The quantum efficiency of the solar cells shown in Fig. 7 give deeper insight into the j_{SC} behavior. At conditions found optimum for the solar cell efficiency (near the transition to a-Si:H growth) the j_{SC} reaches its maximum values at SCs of 4–6% yielding a similar quantum efficiency. The solar cell produced with SC of 7% (dashed line) has a significantly lower long wavelength spectral response ($\lambda > 700$ nm), which can be attributed to the high amorphous volume content. The efficiency for short wavelengths $\lambda < 600$ nm is also reduced. This may be related to a different structure of the p-layer grown onto this i-layer, containing a higher amorphous volume fraction. The solar cells prepared at SCs of 2% and 3% exhibit a carrier extraction problem. The quantum efficiency is strongly reduced, especially at SC = 2%, and shows a characteristic bend around $\lambda = 600$ nm.

Material studies have shown, that higher discharge powers shift the transition to the amorphous growth regime towards higher silane concentrations. To investigate the corresponding influence on the solar cell properties a series of 1 μm thick nip devices has been prepared at different plasma powers and silane concentrations for the

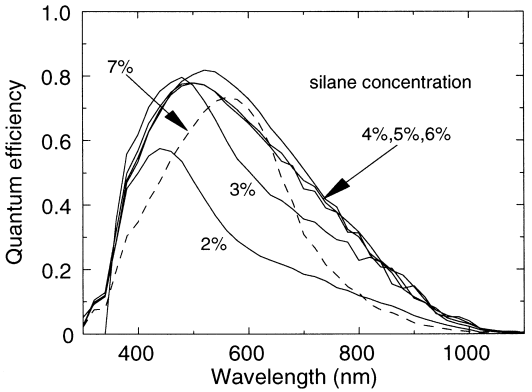

Fig. 7. Quantum efficiency of 1 μm thick *nip* μc-Si:H solar cells. The silane concentrations used for the deposition of the absorber layer are indicated. The corresponding short-circuit current densities are given in Fig. 6(d).

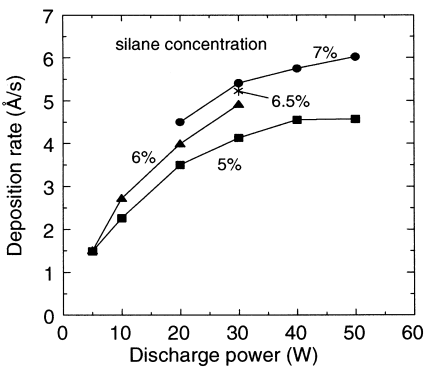

Fig. 8. Deposition rate for i-layers in μc-Si:H solar cells as a function of the applied plasma discharge power.

i-layer. Fig. 8 shows the deposition rates as function of the discharge powers for different SCs. For each SC the deposition rate saturates at high power. This can either be attributed to a power coupling effect, i.e. the increased power fed in by the generator is not dissipated within the plasma (losses in other system components) or to a depletion of silane within the gas phase. This means even higher deposition rates can be expected after improving the reactor design, which will be of technological importance in view of an industrial process. In our experiment deposition rates up to 6 Å/s have already been achieved.

In Fig. 9 the properties of the corresponding solar cells are shown. The filled circles show the data for a silane concentration of 5%. This material has good properties at a low power of 5 W (see Fig. 6). At higher discharge powers all performance values decrease (circles and solid lines). This effect can be partly compensated by increasing

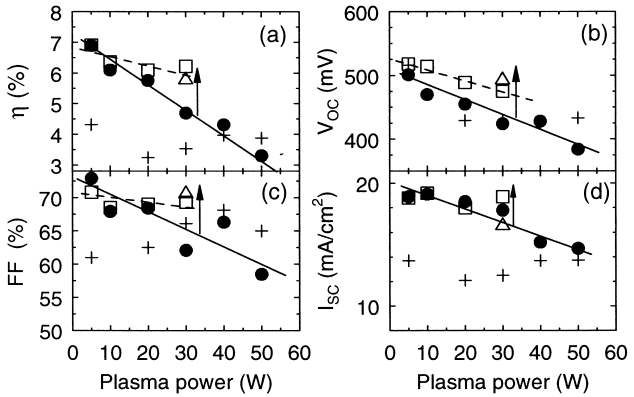

Fig. 9. Results of the I–V measurements of 1 μm thick *nip* solar cells prepared at different plasma powers and silane concentrations. (a) Efficiency η (b) open-circuit voltage V_{OC} (c) fill factor FF (d) short-circuit current I_{SC}. (silane concentrations: (●) 5%, (□) 6%, (Δ) 6.5%, (+) 7%)

the silane concentration. At SC = 6% (open squares and dashed lines) V_{OC} and fill factor are maintained at a high level up to a power of 30 W (arrow markers). As result a good efficiency of 6.2% is achieved at a deposition rate of 5 Å/s. A further increase of SC up to 6.5% (triangles) results in a further improvement of V_{OC} (494 mV) and FF (70.7%). However, the short-circuit current density is reduced and thus the efficiency is not further improved. This loss of j_{SC} with increasing SC is not fully understood yet. Since the electrical properties of the solar cells (V_{OC} and FF) are still good, this effect might be caused by a loss of absorption volume due to a significant amorphous volume fraction within the intrinsic absorber layer. This is consistent with the observation, that at even higher SC = 7% (cross markers) j_{SC} breaks down to approximately 12 mA/cm^2. In this case also V_{OC} and FF are strongly reduced indicating that the transition to amorphous growth has already been crossed.

So far all solar cells had a thickness of 1 μm. For an efficiency optimization the thickness of the active layer was varied. As we reported before [4] in our experiment an increased thickness results in reduced FF and V_{OC}, which is probably caused by limitations of the intrinsic material. As a second effect j_{SC} increases due to enhanced light absorption. These two contrary effects cause only a weak thickness dependency of the solar cell efficiency. Fig. 10 shows the I–V curves of as-deposited solar cells, prepared at a SC of 5% and a plasma power of 5 W with optimized thickness. The *pin* μc-Si:H solar cell with a thickness of 2 μm shows an efficiency of $\eta = 7.5\%$, which is slightly more than the 7% obtained at 1 μm i-layer thickness.

The most promising application of μc-Si:H solar cells is their incorporation as infrared absorber in stacked solar cells. As an example μc-Si:H solar cells, prepared under the conditions found optimum as described above, were applied to prepare a-Si:H/μc-Si:H tandem cells. In this type of device the thickness of both component cells has to be adapted to achieve the maximum efficiency.

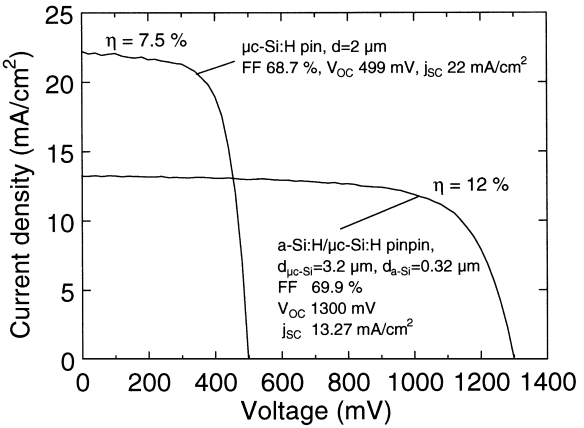

Fig. 10. *I–V* curves of the best performing μc-Si:H *pin* single solar cell and a-Si:H/μc-Si:H *pinpin* stacked solar cell.

In Fig. 10 the I-V characteristics of a *pinpin* tandem device with 3.2 μm μc-Si:H bottom and a 320 nm a-Si:H top cell is shown. The initial efficiency is 12%.

5. Summary

Microcrystalline silicon prepared by VHF-PECVD has been investigated as a material for active layers in solar cells. Its structural composition, e.g. volume content and spatial distribution of amorphous and crystalline phase within the thin film strongly depends on the preparation conditions. By increasing the silane concentration the structure can be changed from highly crystalline dominated by columnar crystallites towards mainly amorphous growth with small crystalline embeddings. Though the transition is rather abrupt, transport properties change gradually. A decrease of dark and photo conductivity is observed, while the photo to dark conductivity ratio increases. When the material is used as an active layer in μc-Si:H solar cells V_{OC} and FF increase with silane concentration. As an important result the deposition conditions near the transition to amorphous growth have been found to be most beneficial to the solar cell properties. A further increase of silane concentration results in a drastically decrease of short-circuit current I_{SC} and fill factor FF, probably caused by amorphous growth. On the other hand a decrease of silane concentration also reduces FF and j_{SC} and results in lower V_{OC} values. Quantum efficiency measurements indicate, that the carrier extraction is limited in this case. Hence it follows, that the μc-Si:H films exhibiting the highest crystalline volume fraction are not necessarily the most suitable for solar cell applications. At higher plasma powers, which have the advantage of higher growth rates, it is even more important to approach the transition to amorphous growth, since high open-circuit voltages are only achieved there. Finally optimized material was used in a 2 μm thick pin solar cell with an efficiency of

7.5% and as 3.2 μm thick infrared absorber in the bottom cell of an a-Si:H/μc-Si:H stacked solar cell yielding an initial efficiency of 12%.

Acknowledgements

We thank F. Birmans, M. Hülsbeck, W. Reetz, H. Siekmann, S. Wieder and J. Wolff for the contributions to this work. This work was supported by BMBF.

References

[1] J. Meier, H. Keppner, S. Dubail, Y. Ziegler, L. Feitknecht, P Torres, Ch. Hof, U. Kroll, D. Fischer, J. Cuperus, J.A. Anna Selvan, A. Shah, in: J. Schmid, H.A. Ossenbrink, P. Helm, H. Ehmann, E.D. Dunlop (Eds.), Proceedings of the 2nd World Conference on Photovoltaic and Solar Energy Conversion, European Comission, Ispra, Italy, 1998, p. 375.
[2] K. Yamamoto, M. Yoshimi, T. Suzuki, Y. Tawada, T. Okamoto, A. Nakajima, Mater. Res. Soc. Symp. Proc. 507 (1998) 131.
[3] K. Saito, M. Sano, K. Matuda, T. Kondo, T. Nishimoto, K. Ogawa, I Kajita, in: J. Schmid, H.A. Ossenbrink, P. Helm, H. Ehmann, E.D. Dunlop (Eds.), Proceedings of the Second World Conference on Photovoltaic and Solar Energy Conversion, European Comission, Ispra, Italy, 1998, p. 351.
[4] O. Vetterl, P. Hapke, O. Kluth, A. Lambertz, S. Wieder, B. Rech, F. Finger, H. Wagner, Solid State Phen. 67–68 (1999) 101.
[5] O. Kluth, A. Löffl, S. Wieder, C. Beneking, W. Appenzeller, L. Houben, B. Rech, H. Wagner, S. Hoffmann, R. Waser, J.A. Anna Selvan, H. Keppner, Proceedings of the 26th IEEE Photovoltaic Specialists Conference, 1997, p. 715.
[6] B. Rech, S. Wieder, C. Beneking, A. Löffl, O. Kluth, W. Reetz, H. Wagner, Proceedings of the 26th IEEE Photovoltaic Specialists Conference, 1997, p. 619.
[7] M. Tzolov, F. Finger, R. Carius, P. Hapke, J. Appl. Phys. 81 (1997) 11.
[8] F. Finger, P. Hapke, M. Luysberg, R. Carius, H. Wagner, M. Scheib, Appl. Phys. Lett. 65 (1994) 2588.
[9] M. Luysberg, P. Hapke, R. Carius, F. Finger, Philos. Mag. A 75 (1997) 31.
[10] L. Houben, M. Luysberg, P. Hapke, R. Carius, F. Finger, H. Wagner, Philos. Mag. A 77 (1998) 1447.
[11] C.C. Tsai, in: H. Fritzsche (Ed.), Amorphous Silicon and Related Materials, World Scientific, Singapore, 1988, p. 123.
[12] P. Hapke, F. Finger, J. Non-Cryst. Solids 227–230 (1998) 861.
[13] J. Meier, P. Torres, R. Platz, S. Dubail, U. Kroll, J.A. Anna Selvan, N. Pellaton Vaucher, Ch. Hof, D. Fischer, H. Keppner, A. Shah, K.-D. Ufert, P. Giannoulès, J. Koehler, Mater. Res. Soc. Symp. Proc. 420 (1996) 3.
[14] F. Finger, J. Müller, C. Malten, H. Wagner, Philos. Mag. B 77 (1998) 805.